Multiwavelength-Integrated Optical Beamformer Based on Wavelength Division Multiplexing for 2-D Phased Array Antennas

Maurizio Burla, *Member, IEEE*, David A. I. Marpaung, *Member, IEEE*, Leimeng Zhuang, *Member, IEEE*, Muhammad Rezaul Khan, *Student Member, IEEE*, Arne Leinse, Willem Beeker, Marcel Hoekman, René G. Heideman, and Chris G. H. Roeloffzen, *Member, IEEE*

***Abstract*—A novel, hardware-compressive architecture for broadband and continuously tunable integrated optical true-time-delay beamformers for phased array antennas is proposed and experimentally demonstrated. The novel idea consists in employing the frequency-periodic response of optical ring resonator (ORR) filters in conjunction with on-chip wavelength division multiplexing (WDM), in order to create multiple signal paths on an individual beamformer channel. This novel idea dramatically reduces the network complexity and, in turn, its footprint on the wafer. This allows the integration of an unprecedented number of delay channels on a single chip, ultimately overcoming the main limitation of integrated optical beamformers, that is, the difficulty to feed antenna arrays with many elements using a single integrated chip. A novel beamformer has been realized based on this technique, using the ultra-low-loss TriPleX waveguide platform with CMOS-compatible fabrication equipment, and its functionality is demonstrated over an instantaneous bandwidth from 2 to 10 GHz. This result, at the best of our knowledge, represents at the same time the record instantaneous bandwidth (8 GHz) for an optical beamformer based on ORR, and the first demonstration of an integrated beamformer where the periodic response of ORRs is exploited to process signals from different antenna elements, simultaneously, using a single delay line.**

Manuscript received January 15, 2014; revised June 4, 2014; accepted June 4, 2014. Date of publication June 22, 2014; date of current version September 1, 2014. This work was supported by the framework of the MEMPHIS project, and Dutch Point One R&D Innovation Project PNE101008, and the Smart Mix Program of the Netherlands Ministry of Economic Affairs and the Netherlands Ministry of Education, Culture and Science, and Agentschap NL, respectively.

M. Burla was with the University of Twente, 7522 NB Enschede, The Netherlands. He is now with the Institut National de la Recherche Scientifique, Montréal, QC H5A 1K6, Canada (e-mail: maurizio.burla@emt.inrs.ca).

D. A. I. Marpaung was with the University of Twente, 7522 NB Enschede, The Netherlands. He is now with the Centre for Ultrahigh Bandwidth Devices for Optical Systems, University of Sydney, NSW 2006, Australia (e-mail: d.marpaung@physics.usyd.edu.au).

L. Zhuang was with the University of Twente, 7522 NB Enschede, The Netherlands. He is now with Monash University, Victoria 3800, Australia (e-mail: leimeng.zhuang@monash.edu).

M. R. Khan was with the University of Twente, 7522 NB Enschede, The Netherlands. He is now with the Islamic University of Technology, Dhaka, Gazipur 1704, Bangladesh (e-mail: m.r.h.khan@utwente.nl).

A. Leinse, M. Hoekman, and R. G. Heideman are with the LioniX B.V., 7521 AN Enschede, The Netherlands (e-mail: a.leinse@lionixbv.nl; m.hoekman@lionixbv.nl; r.g.heideman@lionixbv.nl).

W. Beeker was with the LioniX B.V., 7521 AN Enschede, The Netherlands. He is now with Cambridge Design Partnership, Cambridge, CB23 2RF, U.K. (e-mail: W.P.Beeker@lionixbv.nl).

C. G. H. Roeloffzen is with the University of Twente and Satrax B.V., 7522 NH Enschede, The Netherlands (e-mail: c.g.h.roeloffzen@utwente.nl).

Color versions of one or more of the figures in this paper are available online at http://ieeexplore.ieee.org.

Digital Object Identifier 10.1109/JLT.2014.2332426

***Index Terms*—Microwave photonics, optical beamforming, optical delay lines, phased arrays, resonators, tunable delay.**

I. Introduction

INTEGRATED microwave photonics (IMWP) is a novel field in which the fast-paced progress in integrated optics is harnessed to provide breakthrough performance to well established microwave photonic processing functions, traditionally realized with discrete optoelectronic components [1], [2]. A field where IMWP can have a strong impact is the one of optically controlled antennas. Phased array antennas offer a number of attractive characteristics, including conformal profile, electronic beamforming (beam shaping and beam steering), interference nulling and the capability to generate multiple simultaneous antenna beams. In many cases, however, the performance of a phased array is limited by the characteristics of the beamforming network (BFN) used. It is generally desired—but also difficult—to realize electronic beamformers with broad instantaneous bandwidth, continuous amplitude and delay tunability and, at the same time, capable of feeding large arrays [3]. For this reason, a large amount of research has been directed over the years to optical beamforming. Photonic solutions have shown high performance in terms of operating frequency and bandwidth, but are often bulky, costly, power-hungry, and with low flexibility, since they are generally based on bulk optics and discrete standard optoelectronic devices. Those drawbacks practically limited the diffusion of optical beamforming in real life applications and contributed in reducing the interest in optical beamforming in the past decade. Nonetheless, IMWP solutions have shown the possibility to realize low-loss, low-power, compact and lightweight processors, and to strongly reduce their unit cost thanks to the high yield and reproducibility of the CMOS compatible production process, while retaining or improving the performance. This important perspective paves the way towards extending the application of smart antennas to domains where size and weight are critical (e.g., aerospace, portable devices, access networks, etc). Therefore, integrated photonic beamformers appear to be a promising solution when high performance and reconfigurability is also needed. In line with this approach, in our previous works [4], [5] we have proposed a number of broadband integrated beamformers realized with photonic integrated circuits, using a delay unit based on optical ring resonators (ORR), combiners, and an optical

sideband filter (OSBF) used to generate optical single-sideband modulation (OSSB). Recently, these chips successfully demonstrated squint-free operation for DVB-S satellite reception [4]. However, these integrated solutions still cannot offer the high degree of parallelism of bulk optics, where the control signals for many antenna elements (AE) can be processed simultaneously by the same optical device, to feed thousands of AEs independently [6]. In this case, even using a binary-tree topology [4], [5], a programmable OBFN may become very complex, especially considering the total number of tuning elements required for chip control, and are practically limited to a low number of AEs (up to 16 demonstrated in [7]) or must rely on multiple chips [8].

Over the years, several hardware-compressive techniques have been proposed to improve the capability of optical beamformers to feed large arrays [9]. Solutions based on free-space optics have been demonstrated, employing polarization switches and spatial light modulators (SLM) based on liquid crystals to realize thousands of independently addressable delay lines in parallel, employing a single device [6], [10]. Other hardware-compressive techniques are based on the use of wavelength division multiplexing (WDM) to implement multiple delays on a single delay line and feed multiple antenna elements. These are typically based on dispersive delay elements such as fiber Bragg gratings (FBG) operated in reflection [11], where different wavelengths experience different values of group delay. The main drawback of these solutions is their bulk, as large arrays require long fibers to generate large delays, the need of a circulator that adds complexity and extra loss, limited delay flatness in band and high sensitivity to temperature variations. The integrated optical BFNs reported to date have the advantage of higher compactness, stability and reliability, but offer a limited degree of parallelism, since a separate signal path is required for each antenna element.

In this paper, a novel hardware-compressive network architecture is proposed that introduces parallelism on-chip. The WDM technique and the frequency-periodic characteristic of the ORRs [4] are exploited to achieve multiple delays on a single beamformer channel [12]. Similarly to architectures based on dispersive delay elements, a *single* delay line implements different delay values to feed multiple antenna elements. In turn, this allows a dramatic reduction of the number of required ORRs and, correspondingly, of the network area (almost a factor 10 already for a 16 $\times$ 16-element array) therefore removing the main limitation of integrated optical beamformers. The idea has been translated into an actual layout, and the resulting multi-wavelength beamformer has been fabricated and tested in its basic functionalities. The use of this novel technique, in conjunction with high index contrast waveguides in TriPleX technology, further reduces chip footprint and provides a two-fold advantage, that is, (*i*) it allows to use integrated OBFNs to feed large arrays, and/or to reuse the ORRs for broadening the instantaneous bandwidth [4], as demonstrated in this work, and (*ii*) enables multi-beam applications.

This work is an expanded version of the work presented in [13]. The analysis of the complexity reduction is described in full detail, including a table displaying the improved performance of our solution. The functionality of the main building blocks is thoroughly described, including a detailed schematic of each subsystem and of the overall layout. The experimental characterization of the chip has been completed with new measurements, including the full optical characterization of the on-chip demultiplexer by means of new tests conducted on a separate chip. Fabrication details and design tradeoffs are included, together with new pictures of the chip and the measurement setup. Finally, we describe the electrical and optical tests required for chip selection; we suggest a strategy to choose the parameter variations to maximize the yield; we describe the techniques employed and the setup required for the optical characterization of the chip.

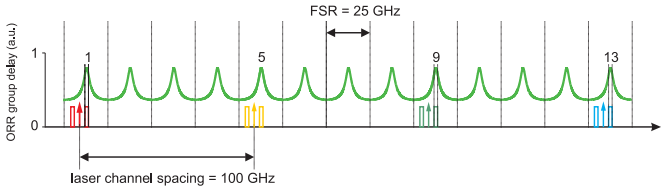

Fig. 1. The periodic response of the ORRs is exploited to delay multiple wavelength-multiplexed signals (from [13]).

The paper is organized as follows. Section II introduces the novel idea and the theory of operation of the proposed multi-wavelength (MWL) beamformer, including a detailed analysis of the asymptotic complexity reduction. Section III describes the system architecture, the operating principle and the characteristics of the main OBFN subsystems. Section IV shows the chip layout and explains the optical test procedure. In Section V the measurement setup is described and the experimental results are displayed and discussed. Section VI gives the conclusions.

II. Theory

A. Multi-Wavelength Beamformers

Optical delay lines (ODL) are fundamental components for a number of all-optical and microwave photonic signal processors. Rasras *et al.* [14] proposed the use of optical ring resonators (ORR) to implement continuously-tunable ODLs. The operating principle has been described extensively in our previous works [4], [5], [7], where we have shown complete optical beamformers based on this concept. Here we present a breakthrough idea that allows a dramatic reduction of complexity. It exploits the frequency periodicity of the ORRs optical response [12], characterized by a periodically-repeating group delay response over frequency, with a period equal to the free spectral range (FSR) of the ORR (see Fig. 1). This characteristic introduces a very large number of "delay bands" with equal group delay, which can be exploited to reuse the same physical delay line for many times, providing a dramatic reduction of complexity. Thus, instead of having a separate delay line for each AE, the idea is to optically multiplex signals originating from different AEs on separate optical carriers (wavelength division multiplexing, WDM) with frequency spacing equal to the FSR (or an integer multiple), and use a single delay line to process as many WDM multiplexed signals as desired. This concept is applicable to all arrays with

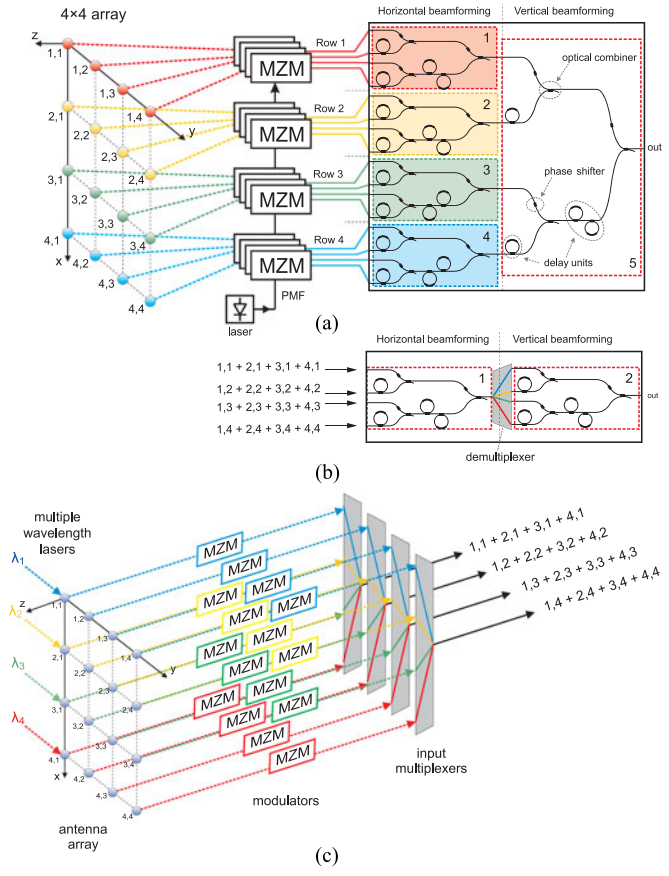

Fig. 2. 4×4 array with separable illumination and corresponding beamformer (a), compared to the MWL-OBFN (b). Note the dramatic reduction in the number of ORRs, area and heaters required. Block diagram representing the connection between the 4×4 array and the MWL-OBFN (c).

separable illumination [3], which is a very common case in practical applications. In this type of array, the array factor can be defined by separately specifying the relative delays among the vertical subarrays (therefore providing horizontal beamsteering, since each of them can be considered as a single element of a horizontal 4×1 array) and between the horizontal subarrays (therefore providing vertical beamsteering, since each horizontal subarray can be considered as a single element of a vertical 4×1 array) [15]. The physical meaning of this concept can be more easily shown by the following example.

In [7] we proposed a planar beamformer used to feed a planar array of 16 elements with separable illumination. This beamformer is based on a binary tree structure, as in Fig. 2(a). The network consists of two sections, the first composed by 4 binary tree stages with four inputs each (labeled "1" through "4" in Fig. 2(a)), used to feed the antenna rows, and the second (labeled "5") including a single 4×1 binary tree stage that provides the desired delay relation among the columns. During operation, the Sections I–IV have all the same delay settings, since it is the relation between the vertical subarrays that determines the horizontal beamsteering. For this reason, they could be conceptually reduced to a single 4×1 binary tree (labeled "1" in Fig. 2(b)) where the signals are being multiplexed. This is possible by employing WDM in conjunction with the frequency

TABLE I
ASYMPTOTIC COMPLEXITY COMPARISON BETWEEN SWL AND MWL-OBFN

N	Nr. AEs	Nr. ORR /sec.	Nr. sections (SWL)	Total nr. ORRs (SWL)	Nr. sections (MWL)	Total nr. ORRs (MWL)
2	4	3	3	3	2	2
4	16	4	5	20	2	8
8	64	12	9	108	2	24
16	256	32	17	544	2	64
...	...	...	...	...	...	...
N	$N2$	$(N/2)\log_2(N)$	$N+1$	$(N+1)(N/2)\log_2(N)$	2	$2(N/2)\log_2(N)$

Asymptotic complexity comparison between the single-wavelength and multi wavelength OBFN architectures. (Assumptions: N is a power of 2; antenna array planar and square ($N \times N$); separable illumination)
$N =$ nr. of antenna elements on each side of the square array. $\mathrm{ORR_{SWL}} =$ Nr. ORRs (SWL) = (nr. of sections, SWL × ORRs/section). $\mathrm{ORR_{MWL}} =$ Nr. ORRs (MWL) = (nr. of sections, MWL × ORRs/section) = (2 × ORRs/section).

periodic response of ORRs, which is exploited to allocate the wavelength-multiplexed signals in different periods of the ORRs response (see Fig. 1).

B. Complexity Analysis

From the schematic in Fig. 2, it can be seen that the proposed technique allows a dramatic reduction of number of ORRs required with respect to the case of a traditional binary-tree single-wavelength architecture, as the one depicted in Fig. 2(a). This reduction is more sensible for a larger number of elements (see Table I). This is of paramount importance since, in practical implementations, the dominant factor in wafer area occupation is given by the ORRs [4], therefore their number is an accurate indicator of the required die area. For an asymptotic complexity analysis, we assume the realistic assumptions that the array is square ($N \times N$), being N a power of 2, and that 1 ORR is sufficient to create the desired delay among adjacent AEs (as in the cases shown before [4], [5]), it can be shown [16] that the number of ORRs in each OBFN stage is $(N/2)\log_2(N)$. The total number of ORRs equals the ORRs per stage multiplied by the number of stages, that is $N+1$ in single wavelength OBFNs (SWL-OBFN) and only 2 for MWL-OBFN (see Fig. 2(b)). Thus the total number of ORRs for a SWL-OBFN and for a MWL-OBFN are respectively given by the equations

$$\mathrm{ORR_{SWL}} = (N+1)\left[\left(\frac{N}{2}\right)\log_2(N)\right] \in O(N^2 \log_2 N) \tag{1}$$

and

$$\mathrm{ORR_{MWL}} = (2)\left[\left(\frac{N}{2}\right)\log_2(N)\right] \in O(N \log_2 N). \tag{2}$$

The big O notation [17] has been used in (1) and (2) to represent the speed of growth with respect to N. When we plot the two functions versus N, as in Fig. 3, we can see that the reduction of complexity becomes dramatic already for relatively small numbers of AEs. In fact, for a 36 (6×6) elements array, the number of ORRs surpasses 50 (the largest ORR-based OBFN realized so far contains 40 ORRs [7]), corresponding

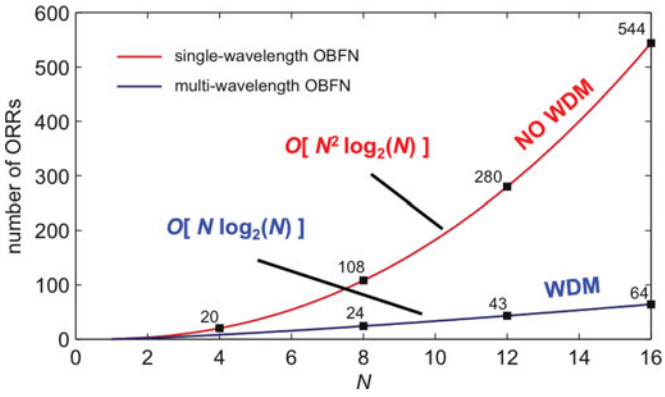

Fig. 3. Number of ORRs versus array dimension, for single-wavelength (red) and multi-wavelength OBFN (blue). N indicates the number of elements on each side of a square antenna array.

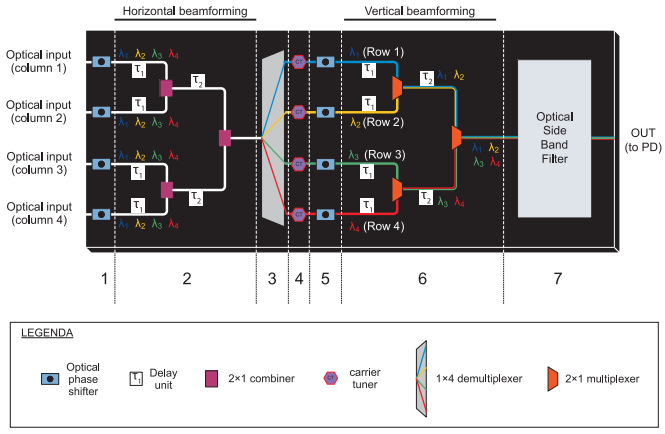

Fig. 4. Schematic representation of the multi-wavelength, multiple-signal-path OBFN, intended to feed a 4×4 planar antenna array.

to over hundred independent control signals, in addition to the tuning elements required for combiners and phase shifters on chip. Employing a MWL-OBFN, instead, the same number of elements could control an array with 256 AEs, which would otherwise require more than 500 ORRs, meaning thousands of control elements on a single chip, which is way beyond the limit of the photonic integration technology currently employed.

The large reduction in number of ORRs required provides, in turn, a reduction in system complexity, in chip area occupation, in power and heat dissipation needed to program and control the beamformer. In addition, the saved area can now be employed to add ORRs for the scope of broadening the instantaneous bandwidth, as demonstrated in the following sections.

Note that in this discussion the presence of the multiplexer and demultiplexer stages, required in the MWL architecture, Fig. 2(b), have been neglected in the complexity calculation. Nonetheless, as will be seen in the following, those components do not include ORRs which are considered in this study as the most impactful elements on the system complexity, in terms of tuning and required die area occupation, and thus have a limited impact on the fractional complexity, especially for large numbers of N which the use of the multi-wavelength technique is aimed for.

III. System Architecture and Operation

A. Basic Sections

The MWL-OBFN is composed by seven cascaded sections, as shown in Fig. 4: (1) Optical phase shifter Section I; (2) Horizontal beamforming section; (3) Optical demultiplexer; (4) SCT section; (5) Optical phase shifter Section II; (6) Vertical beamforming section; (7) Optical sideband filter.

B. Operating Principle

A demonstrator of the MWL-OBFN has been designed according to the schematic shown in Fig. 4 to feed a 16-elements antenna array. The chip has only four inputs, each of them carrying the signals originating from four different antenna elements (for a total of 16 AEs), which are wavelength-multiplexed using different optical carriers with a channel spacing $\Delta f = 100$ GHz. After passing through independent optical phase shifters (1), in the horizontal beamforming section (2), those signals are delayed with respect to each other by the delay units τ_1 and τ_2 (see Fig. 4) and then optically combined. This allows horizontal beamsteering (see also Fig. 2) of the main lobe of the generated antenna pattern. The combined output is then applied to a 1×4 demultiplexer (DEMUX, 3). Each wavelength is used to modulate the signals of the same row (see Fig. 2(c)). As a consequence, each output of the DEMUX carries the combination of signals received by the antenna elements of the same row. Those signals are then applied to the second part of the MWL-OBFN, namely the vertical beamforming section (6), where they are delayed with respect to each other by the delay units τ_1 and τ_2. This operation corresponds to the vertical beamsteering. The horizontal and vertical beamsteering sections have symmetric binary tree architecture. As demonstrated in [19], it can be shown that the choice of using two distinct delay elements τ_1 and τ_2 placed on the binary tree as in Fig. 4 allows to minimize the complexity of the individual delay elements, and ultimately has the effect to reduce the overall network complexity, with respect to the case of using a single independently-tunable delay element per input. An optical side band filter on-chip (7) is used to select only one sideband plus the optical carrier, for each of the laser wavelengths, as shown in Fig. 5.

The filter consists of an asymmetric Mach–Zehnder interferometer loaded with an ORRs on each interferometer arm [18]. The FSR of the filter has been chosen equal to 25 GHz in such a way that the periodic response can be used to filter the four IM carriers (100 GHz apart) simultaneously, as shown in Fig. 5(b). Optical single-sideband (OSSB) modulation is preferred since it allows a strong reduction in the required delay bandwidth [19], and the carrier is kept to allow direct detection of the RF signals. A filter with the same architecture and technology has already been realized and characterized, and the results are reported in [18]. A thorough description of the operation of the delay units is given in [4], [5], [7].

The optical demultiplexer (3) has a binary tree structure based on asymmetric MZIs (AMZIs) [20], with different values of

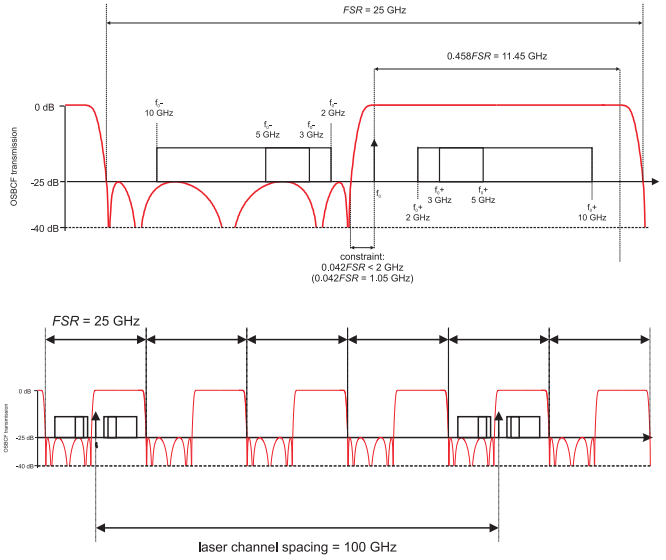

Fig. 5. Simulated response of the OSBF employed for OSSB modulation, in comparison with the optical spectrum (a). The frequency periodic response of the filter is used to filter multiple wavelengths simultaneously (b).

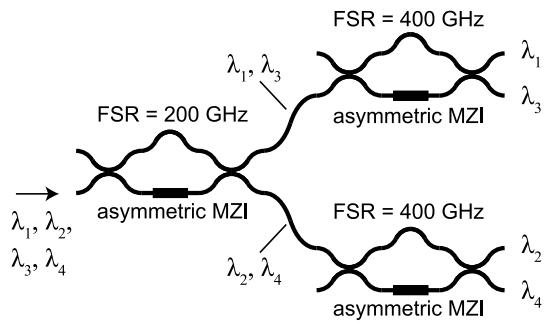

Fig. 6. Block diagram of the 1×4 demultiplexer.

FSR, as shown in [21]. The FSR of an AMZI is determined by the difference in path length between the branches of the interferometer. The FSR has to be chosen in order to separate the four wavelengths of four lasers (λ_1, λ_2, λ_3, λ_4) that, in our example, have a channel spacing Δf of 100 GHz. The resulting structure and the choice of the FSR for the different AMZIs is shown in Fig. 6.

The demultiplexer is composed of two stages (see Fig. 6). The first stage contains an AMZI with an $\mathrm{FSR} = 200$ GHz, used to separate the four wavelengths into the two couples of channels (λ_1, λ_3) and (λ_2, λ_4). The second stage contains two AMZIs with an $\mathrm{FSR} = 400$ GHz. This will be used to effectively separate the individual wavelengths into the four inputs of the vertical beamformer section, as will be shown in Section V.

A carrier tuner (CT, 4) is placed at each output of the optical DEMUX. It consists of a separate couple of optical ring resonators whose resonant wavelengths will be tuned in such a way to modify the phase of the carrier frequency only, separately from and without affecting the one of the information signal. In particular, the phase of the carrier must be made equal to the one

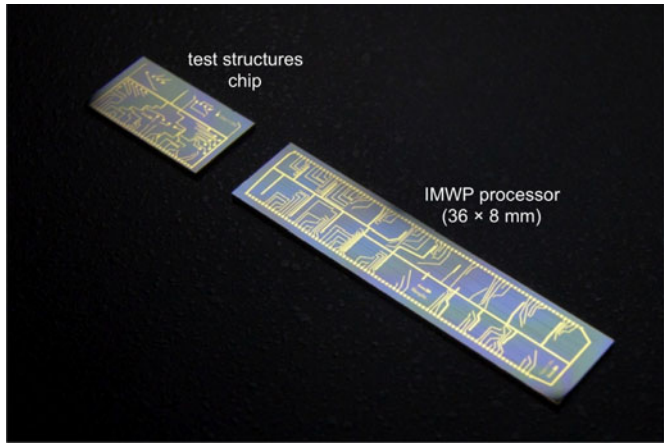

Fig. 7. Picture of the realized chips (MWL-OBFN dimensions: $36 \times 8\ \mathrm{mm}^2$).

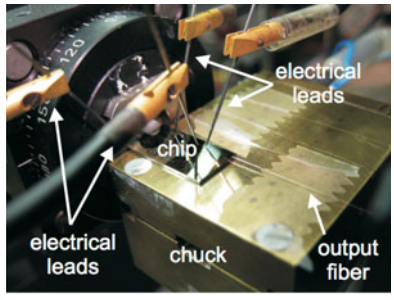

Fig. 8. Test chip on the bare fiber alignment setup. The chuck provides support and heat sink. The chip is kept in place using a vacuum pump.

that it would have experienced in the case in which broadband ideal delays had been used. The concept of SCT using optical ring resonators has been described in detail and experimentally demonstrated in [22].

IV. Chip Schematic and Layout

The functional schematic in Fig. 9 has been translated into a mask layout by LioniX BV, as represented in Figs. 10 and 11. The different sections of the MWL-OBFN processor are made accessible at the external optical interfaces via multiple test ports, for subsystem test purposes (see Fig. 11).

The chip has been fabricated on low-loss TriPleX waveguide technology [18] by LioniX BV. The overall dimension of the fabricated chip is $36 \times 8\ \mathrm{mm}^2$ (see Figs. 7 and 10).

A test chip was also included on the realized mask. A picture of both chips is shown in Fig. 7.

V. Experiment

Experiments were conducted in two stages. First, optical and electrical test of the subsystems were performed in order to verify their correct operation. After that, RF test have been performed to demonstrate the correct functionality of the novel OBFN.

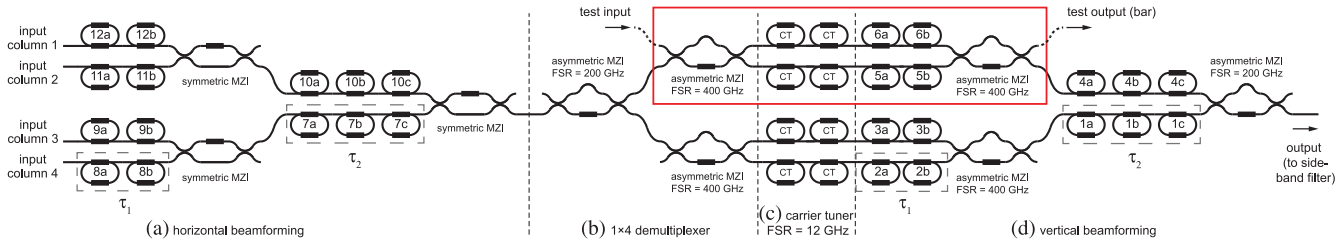

Fig. 9. Schematic representation of the MWL-OBFN. Inset: section used for the RF functionality tests (from [13]).

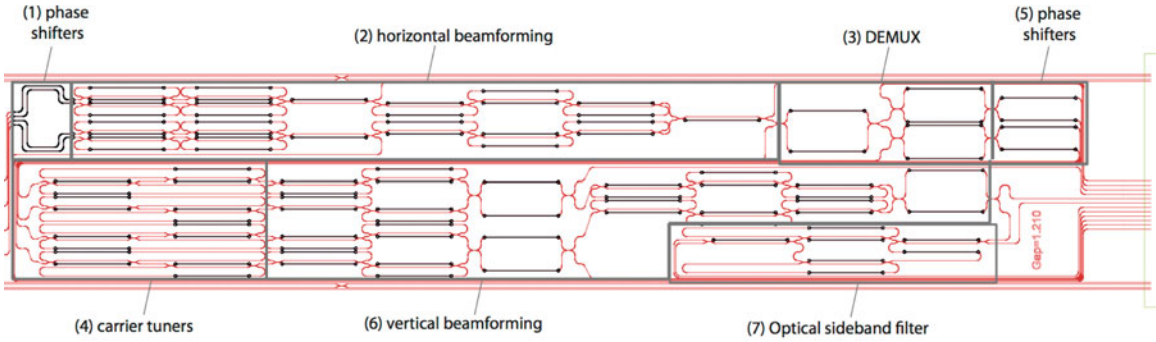

Fig. 10. MWL-OBFN layout (36×8 mm).

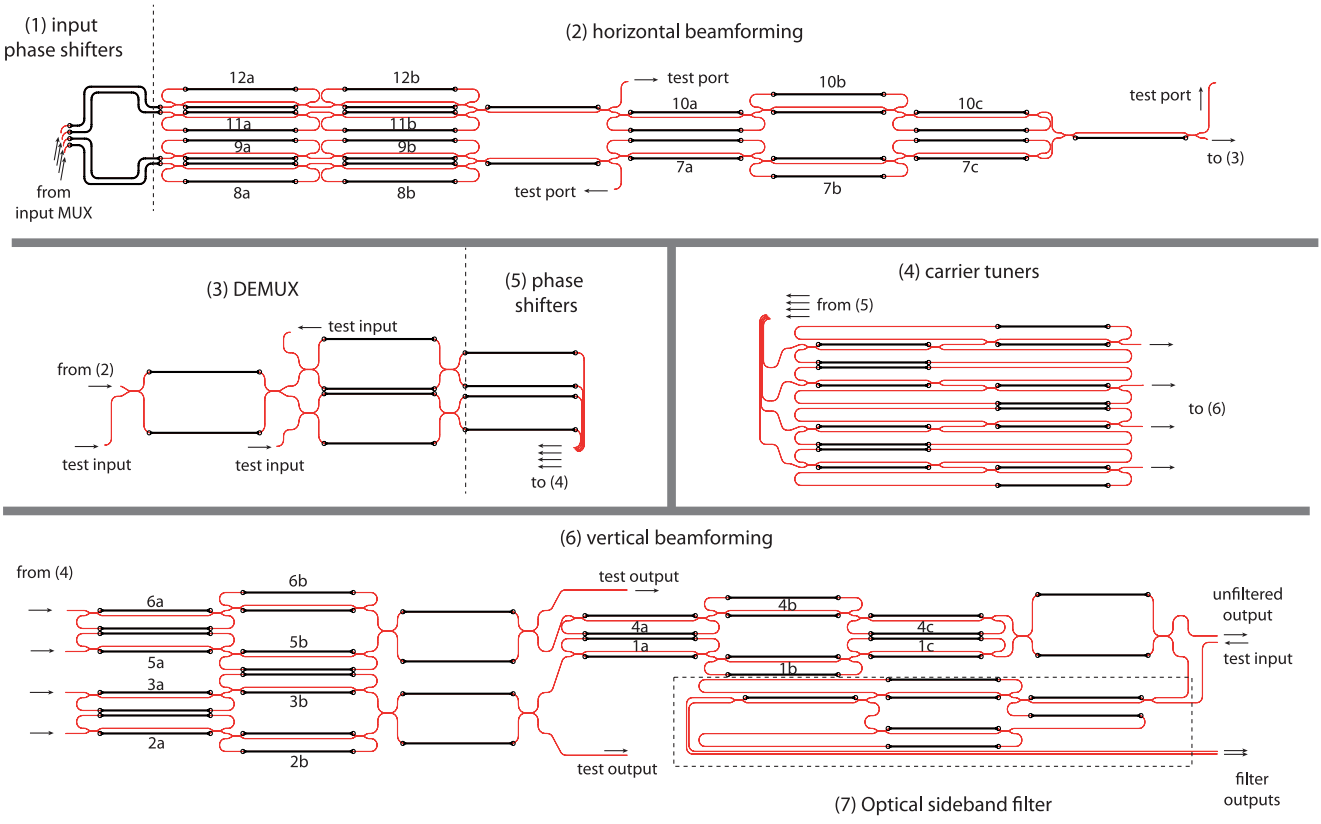

Fig. 11. Detailed layouts of the different sections of the MWL-OBFN. Each section is numbered (in brackets) as in Fig. 4, while the ORRs are labeled as in Fig. 9.

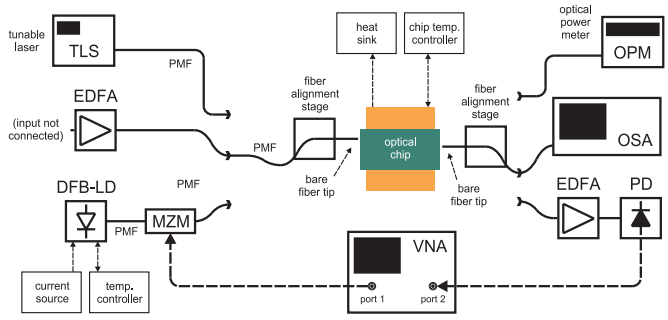

Fig. 12. Setup used for the optical tests.

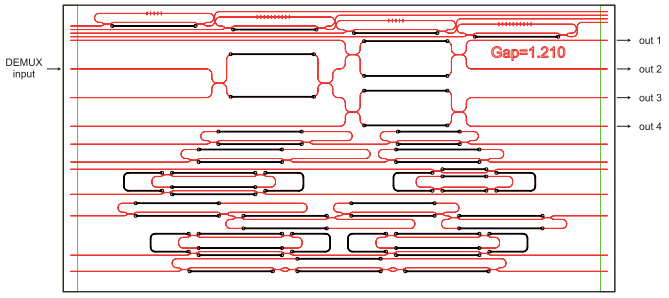

Fig. 13. Layout of the chip with test structures. The input and outputs of the DEMUX are indicated.

A. Initial Tests

After the photonic chips were diced off the wafer, an initial characterization was performed to test the basic chip functionality, and the correct operation of the basic building blocks. This type of test is divided in electrical test and optical test. The electrical tests include the verification of the electrical continuity for each individual control line, the test of the ohmic resistance of the ground lines and the heaters. The optical test starts with the measurement of the fiber-to-chip coupling losses and the test of the main building block, that is, the 50:50 optical directional coupler, and the waveguide loss.

The fiber-to-chip coupling loss was as low as 1.5 dB/facet for this batch of chips, thanks to the introduction of spot-size converters, compared to approximately 6 dB/facet of previous chips. The waveguide mask contains three complete replicas of the whole set of desired structures, which differ only in the coupling gap of the directional couplers contained in the functional structures. One value is the nominal one obtained by simulations, and the other two are chosen as a safety margin to compensate for variations and inaccuracies in the fabrication process. In this case, the gaps were chosen to be 1.094, 1.152 and 1.210 μm. The gap of 1.152 μm turned out to be the one that makes the coupling ratio of the directional couplers closest to the desired value of 0.5. The corresponding chips were selected and used in the following tests.

Another very important parameter that is tested is the waveguide loss. As discussed in [19], the waveguide loss has a very strong impact on the overall system performance of the optical beamformer system. When the structures include optical ring resonators, this test can be conveniently and accurately performed by means of the procedure described in [18]. For this batch, the waveguide loss was measured to be as low as 0.1 dB/cm.

In order to test the optical performance of the tunable structures, it is necessary to access the chip waveguides as well as the electrical contacts of the heaters, while keeping the chip at a controlled temperature. This was done by mounting the optical chip on a copper chuck, which includes thermal control via a Peltier element and a temperature sensor, and by edge-coupling bare fibers to the waveguides to be accessed by using a suitable fiber alignment stage, featuring micrometric three-axis control of the fiber position. Tungsten leads were used to provide electrical control to the heaters. A picture of the test chip mounted in this setup is shown in Fig. 8.

B. Optical Test: Demultiplexer Characterization

Among other structures, the test chip contains an exact replica of the DEMUX included in the complete OBFN chip (see Fig. 13). This device has 2 inputs and 4 outputs that are all accessible using bare fibers and the alignment setup described above and shown in Figs. 8 and 12.

By connecting the tunable laser source (TLS) to the input of the optical chip, and the power meter at one of the outputs, it is possible to measure the optical transmission of the selected input-output path with respect to wavelength, by scanning the wavelength of the laser and measuring the corresponding optical power impinging on the optical power meter (see Fig. 12). This is done using an automated setup controlled via LabView. In the case of the DEMUX, the TLS was connected to the DEMUX input in the left of Fig. 13, and the output bare fiber has been aligned sequentially to each of the outputs for the characterization of each of the four DEMUX channels.

As seen in Fig. 6, the DEMUX is composed of two sections: one consisting of an AMZI with 200 GHz FSR, whose output are connected to the inputs of two AMZI with 400 GHz FSR. Tunable voltages were applied to the heaters that control the phase shifters on the branches of the three AMZIs that form the DEMUX, as visible in Fig. 14. First, the 400 GHz AMZIs are tuned, using the test input ports on the chip visible in Fig. 13; then, the 200 GHz AMZI is tuned. This procedure allowed a fine-tuning of the frequency response of the complete 1×4 DEMUX and a good matching with the desired response. The measurement results are shown in Fig. 15, in comparison with the simulated responses of each DEMUX channel.

From the measurement it can be observed that the positions of the passbands and of the stopbands are matching very well with the simulated ones, for all of the four channels. This is particularly evident by looking at the frequency position of the zeroes of transmission with respect to the simulated response. Nonetheless, as expected, the analysis of the zeroes of transmission shows as well that the depth of the zeroes is not equal across all the DEMUX channels. Specifically, when input 1 of the DEMUX is used, as in this case, channels 3 and 4, which are connected to the input via the cross port of the input AMZI,

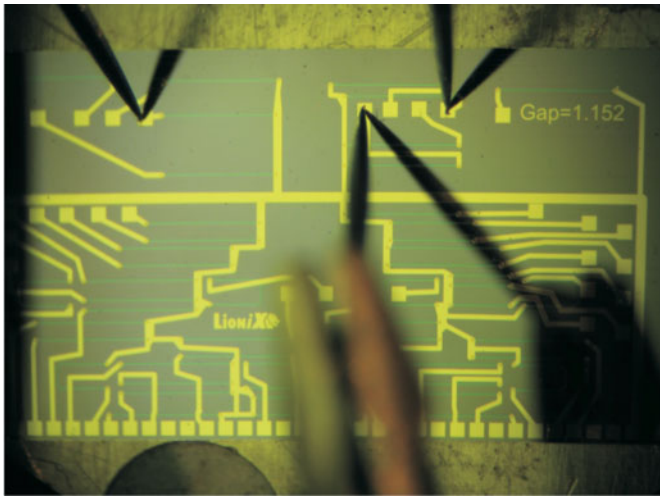

Fig. 14. Chip containing the test structures for the MWL-OBFN, as visible at the optical microscope. The needles are used to draw current through the heaters for tuning the responses of the optical structures.

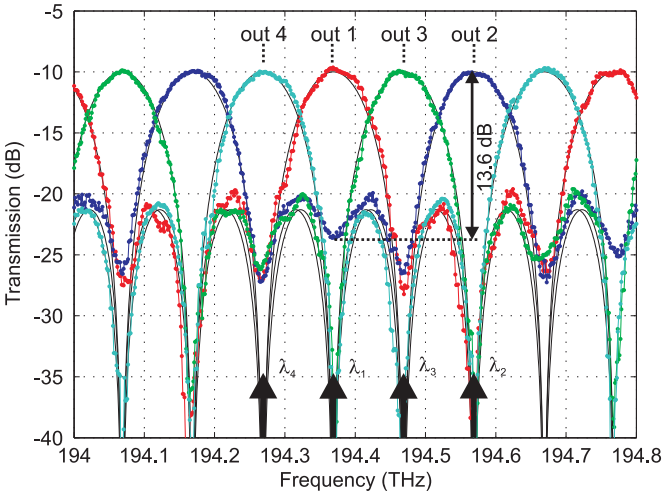

Fig. 15. Measured (dotted lines) and simulated (solid lines) optical transmission of the DEMUX channels 1, 2, 3, and 4.

show a similar performance, both having a high suppression in their stopbands. On the contrary, channels 1 and 2 suffer a lower suppression in stopband, a fact which is particularly visible for channel 2, being this directly connected to the DEMUX input via the bar port of both the first-stage and of the second-stage AMZIs. This translates into a non-perfect suppression of the undesired sidebands, which in the worst case (for port 2) can be as low as 13.6 dB. This non-ideal suppression is due to the fact that the directional couplers employed in the design have still residual variations with respect to their perfect 50:50 splitting ratio; this, in turn, creates an unbalance in the routing of the optical power between the bar and the cross ports, making impossible to route all the optical power from the input to the cross port, thus leaving a residual optical power in the bar port. Nonetheless, the residual power unbalance can be compensated for by

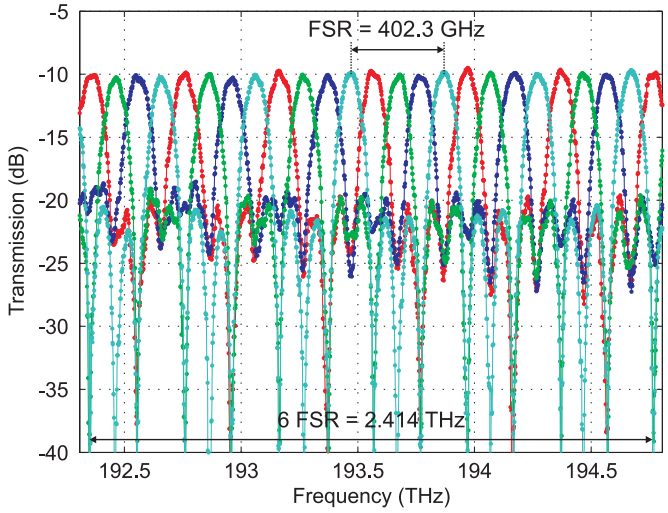

Fig. 16. Measured DEMUX response of channels 1, 2, 3, and 4.

properly adjusting the transmission of the tunable multiplexer in the following vertical beamforming stage of the MWL-OBFN.

Fig. 16 shows the DEMUX response over a wider frequency band. The transmission characteristic keeps a high degree of accuracy over a large bandwidth, making possible to accommodate wavelengths at different central frequencies; this is also a proof that the fabrication procedure is sufficiently accurate and the proposed multi-wavelength approach could be extended to a much larger number of wavelengths. The FSR of the DEMUX can be measured and appears to be 402.3 GHz (99.425% accuracy, 400 GHz by design).

C. RF Tests: Demonstration of Basic Functionalities

The main target of the test described in this section is the demonstration of the basic functionality of the MWL-OBFN, that is, the capability of demultiplexing, selectively delaying and combining RF signals carried by different optical wavelengths. For that purpose we designed and realized a set of tests on a subsection of the MWL-OBFN chip. In particular, the aim is to: (*i*) create two IM signals with different optical carrier frequencies, spaced 200 GHz apart; (*ii*) route the two IM signals to a single input of the MWL-OBFN; (*iii*) de-multiplex the two signals to separate paths on the chip; (*iv*) show the group delay applied selectively to only one of the two signals; and (*v*) demonstrate the multiplexing (combining) of the two signals. For this demonstration, the simplest structure required consists of a 1×2 DEMUX, whose outputs are connected to two separate waveguides, containing independently tunable delay sections, being then combined by a multiplexer (MUX). This structure is schematically represented in Fig. 17(a). Therefore, for this test we employ the chip subsection indicated by the box in Fig. 9. This is the simplest structure available on-chip that contains the basic components required for the test. Such structure can be accessed by two test ports, which have been added by design for this type of tests and have been made available at the output facet of the chip, Fig. 17(b). The proposed

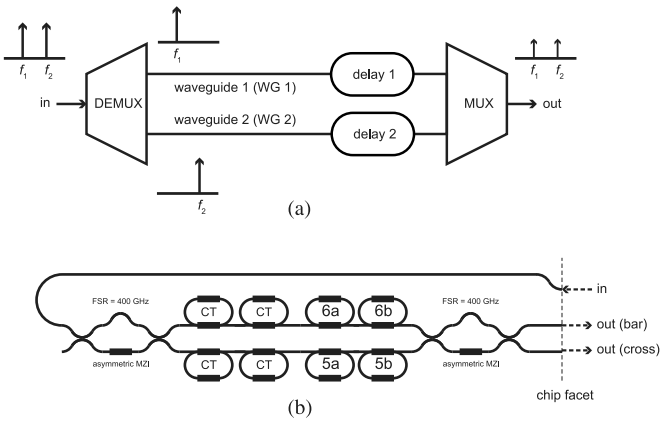

Fig. 17. Schematic of the portion of the MWL-OBFN used for the functionality tests: 1×2 DEMUX, cascaded to two separate waveguides (including separate tunable delay sections), combined by a MUX (a). Corresponding schematic of the selected section on the MWL-OBFN chip (b).

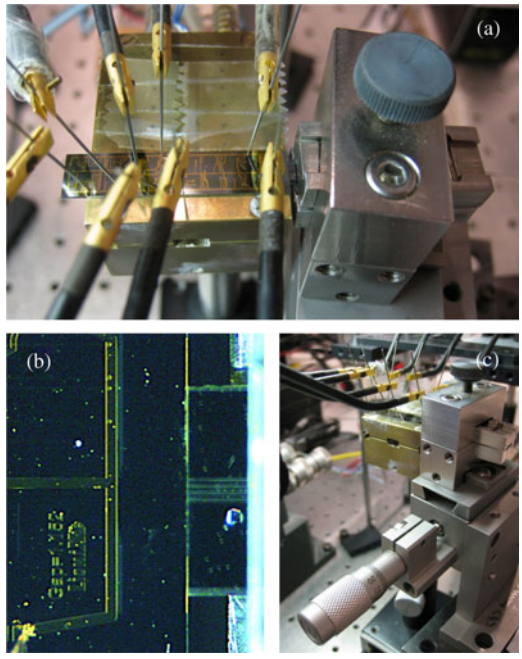

Fig. 18. Alignment stage including the FAU used to access multiple waveguide ports on the right facet of the MWL-OBFN chip (a). The FAU containing 4 fiber pigtails has been aligned to the optical waveguides (b). Note the presence of the goniometer used to align the plane of the fiber array to the plane of the chip (c).

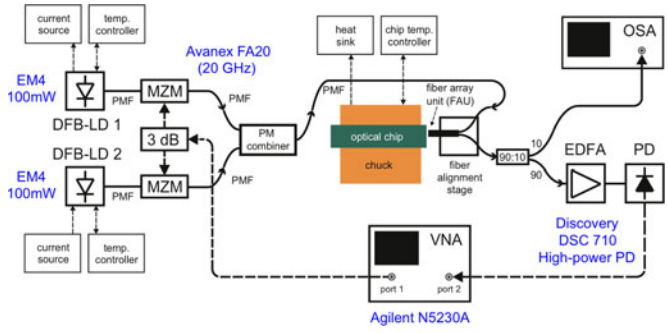

Fig. 19. Setup employed for the basic functionality demonstration of the MWL-OBFN (from [13]).

test requires transmission measurements, thus both ports have to be accessible simultaneously. Nonetheless, the measurement setup shown in Figs. 8 and 12 allows to access only one port per facet at a time. Therefore, the setup has been modified for this specific test by replacing the single bare fiber at the output facet with a fiber array unit (FAU) from OZ Optics Ltd. This FAU includes four polarization maintaining (PM) fibers, whose cores are horizontally spaced 125 um, which corresponds to the pitch separation between the output waveguides on the chip. In this way, a single FAU could be used to access as many as four adjacent ports of the output facet simultaneously. Since the desired test ports are adjacent, the 4-fibers FAU is sufficient for the desired test.

The FAU has been mounted on a goniometer, used to align the plane of the chip with the plane of the fiber pigtails of the FAU and maximize the optical transmission between the test ports. Fig. 18 shows a picture of the alignment stage including the goniometer and the FAU. Fig. 19 shows the employed measurement setup. Two EM4 high power laser (DFB-LD 1 and DFB-LD 2, 100 mW each, in 1550 nm band) provide two optical carriers (f_1 and f_2) spaced 200 GHz apart, which are intensity modulated (IM) by the RF signal generated by an Agilent N5230A vector network analyzer (VNA), using two Avanex FA20 Mach–Zehnder modulators (MZM) biased in quadrature. The signals are combined and fed to the optical chip in Fig. 10 for signal processing. An erbium doped fiber amplifier (EDFA) is used to compensate for the fiber to chip coupling losses. The RF output of a Discovery DSC 710 high-power photodetector (PD) is connected to port 2 of the VNA for the amplitude and phase measurements.

D. Demultiplexing

Fig. 20 shows the s_{21} parameter, measured over the band 50 MHz-10 GHz, of the bar response of the MWL-OBFN system under test (see Fig. 19), when only one laser at a time is connected to the PM combiner inputs. The RF powers have been equalized while keeping the optical frequencies at the desired values, by tuning both the drive current and the operating temperature of each DFB laser. Note the gain roll-off with frequency, due only to the electro-optical response of the MZM and of the PD employed, the losses of the multiple RF connectors, adapters, and of the coaxial cables employed in the setup. The observed roll-off does not depend upon the insertion of the chip in the photonic link. The delay characteristics show an initial delay difference among the paths of approximately 38.1 ps. The delay difference can be fully programmed using the on-chip ORRs, as will be shown in Section F.

E. Channels Combining

When both lasers are connected to the PM combiner, the two modulated signals are coupled via a single fiber to the chip, where they are demultiplexed, processed (individually delayed)

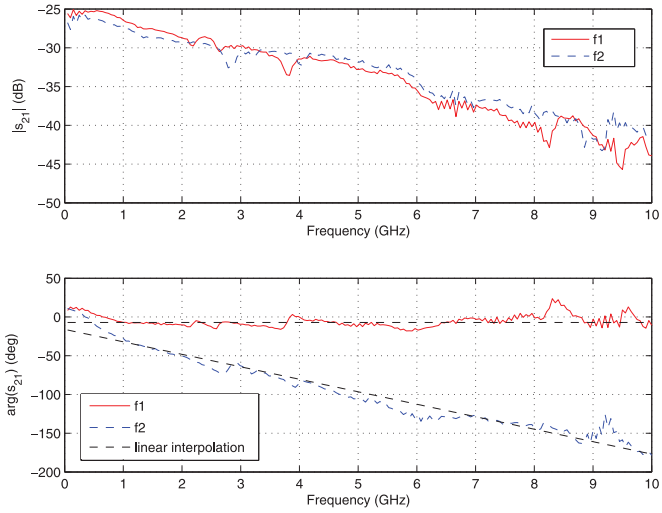

Fig. 20. RF magnitude and phase response of channels 1 and 2 (from [13]).

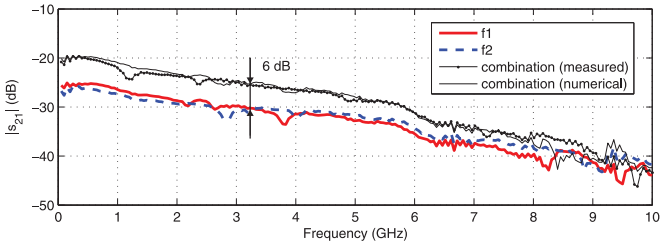

Fig. 21. RF magnitude and response of channel 1, channel 2, and their combination on-chip (from [13]).

and then recombined. The RF magnitude response shows a corresponding increase of 6 dB with respect to the individual channels (see Fig. 20). In fact the two electrical signals, which are carried separately in the optical domain by the different wavelengths, are converted back to the electrical domain at the PD. At the PD output, the RF signals sum in phase, producing a total electrical signal with double amplitude, thus four times the RF instantaneous power (6 dB), as shown in Fig. 21. This result demonstrates the combining capability of the proposed MWL-OBFN.

Observing the response, it can be noted that the power of the combined response decreases faster with frequency than the ones of the individual channels, producing only a 3 dB increase around 7 GHz, and no increase around 10 GHz. This can be easily explained by considering that the conclusion of coherent RF combining drawn before is valid only as long as the frequency is sufficiently low to consider two RF signals approximately in phase. In fact, as visible from the phase responses in Fig. 20, the two waveforms have a small delay difference of approximately 38 ps. This limited amount of delay produces a phase shift between the two detected RF signals which is negligible below few GHz but, as the frequency increases, the delay starts to play a significant role (i.e., to produce a substantial phase shift between the RF signals) until, around 13 GHz,

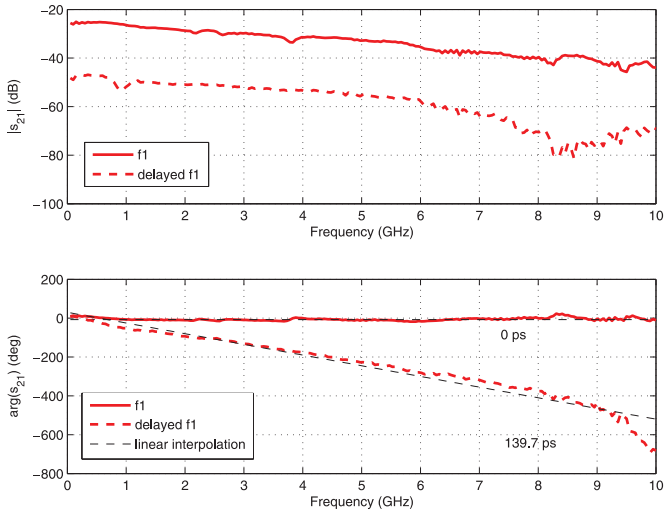

Fig. 22. RF magnitude and phase response of channel 1 compared to the response of channel 1 delayed (from [13]).

the two waves are completely out of phase. If we could extend the RF sweep, we would see that this phenomenon produces an interference pattern characteristic of a microwave photonic filter [2]. In this case, the FSR of this filter would be equal to $1/(38.1\ \text{ps}) = 26.247\ \text{GHz}$.

F. Selective Delay

After the demonstration of the combining capability of the MWL-OBFN, we show the capability to generate selective delay to only one of the IM optical signals. For this scope, the ORRs of WG 1 in Fig. 17 labeled as "6a" and "6b" have been employed to provide broadband delay to the IM signal at frequency f_1. Fig. 22 shows the RF phase response obtained when only DFB-LD 1 (f_1) is connected to the chip, for two different delay settings. The phase response obtained when DFB-LD 2 is connected stays substantially unchanged. This demonstrates the capability of the chip to provide broadband delay, selectively to the RF signal modulated on the optical carrier at frequency f_1. The delay is continuously tunable from 0 ps up to approximately 139.7 ps over a record instantaneous bandwidth of 8 GHz thanks to the increased number of ORRs per delay line allowed by the complexity reduction. Note the attenuation on the RF amplitude response due to the application of the delay, which can be compensated by properly adjusting the optical power of the corresponding laser.

REFERENCES

[1] D. Marpaung *et al.*, "Integrated microwave photonics," *Laser Photon. Rev.*, vol. 7, pp. 506–538, Jul. 2013.
[2] J. Capmany, J. Mora, I. Gasulla, J. Sancho, J. Lloret, and S. Sales, "Microwave photonic signal processing," *IEEE J. Lightw. Technol.*, vol. 31, no. 4, pp. 571–586, Feb. 2013.
[3] R. J. Mailloux, *Phased Array Antenna Handbook*. New York, NY, USA: Artech, 2005.
[4] L. Zhuang, C. G. H. Roeloffzen, A. Meijerink, M. Burla, D. A. I. Marpaung, A. Liense, M. Hoekman, R. G. Heideman, and W. van Etten, "Novel ring resonator-based integrated photonic beamformer

for broadband phased array receive antennas—Part II: Experimental prototype," *IEEE J. Lightw. Technol.*, vol. 28, no. 1, pp. 19–31, Jan. 2010.

[5] M. Burla, D. A. I. Marpaung, L. Zhuang, A. Liense, M. Hoekman, R. G. Heideman, and C. G. H. Roeloffzen, "Integrated photonic K_u-band beamformer chip with continuous amplitude and delay control," *IEEE Photon. Technol. Lett.*, vol. 25, no. 12, pp. 1145–1148, Jun. 2013.

[6] D. Dolfi, F. Michel-Gabriel, S. Bann, and J. Huignard, "Two-dimensional optical architecture for time-delay beam forming in a phased-array antenna," *Opt. Lett.*, vol. 16, pp. 255–257, 1991.

[7] M. Burla *et al.,* "System integration and radiation pattern measurements of a phased array antenna employing an integrated photonic beamformer for radio astronomy applications," *Appl. Opt.*, vol. 51, pp. 789–802, 2012.

[8] D. Marpaung *et al.,* "Development of a broadband and squint-free Ku-band phased array antenna system for airborne satellite communications," in *Future Aeronautical Communications*, Rijeka, Croatia: Intech, 2011, pp. 201–224.

[9] N.A. Riza, *Selected Papers on Photonic Control Systems for Phased Array Antennas*. Bellingham, WA, USA: SPIE, vol. MS136, 1997.

[10] N. A. Riza and N. Madamopoulos, "Characterization of a ferroelectric liquid crystal-based time delay unit for phased array antenna applications," *IEEE J. Lightw. Technol.*, vol. 15, no. 7, pp. 1088–1094, June 1997.

[11] J. Corral, J. Marti, S. Regidor, J. Foster, R. Laming, and M. Cole, "Continuously variable true time-delay optical feeder for phased-array antenna employing chirped fiber grating," *IEEE Trans. Microw. Theory Tech.*, vol. 45, no. 8, pp. 1531–1536, Aug. 1997.

[12] M. Burla *et al.,* "Multiwavelength optical beam forming network with ring resonator-based binary-tree architecture for broadband phased array antenna systems," in *Proc. LEOS Benelux Symp.*, Nov. 27–28, 2008, Enschede, The Netherlands, pp. 99–102.

[13] M. Burla, Z. Leimeng, D. Marpaung, M. R. Khan, A. Leinse, W. Beeker, M. Hoekman, R. Heideman, and C. Roeloffzen, "On-chip, CMOS-compatible, hardware-compressive integrated photonic beamformer based on WDM," presented at the IEEE Int. Topical Meeting Microw. Photon., Oct. 28–31, 2013, Alexandria, VA, USA.

[14] M. S. Rasras, C. K. Madsen, M. A. Cappuzzo, E. Chen, L. T. Gomez, E. J. Laskowski, A. Griffin, A. Wong-Foy, A. Gasparyan, A. Kasper, J. Le Grange, and S. S. Patel, "Integrated resonance-enhanced variable optical delay lines," *IEEE Photon. Technol. Lett.*, vol. 17, no. 4, pp. 834–836, Apr. 2005.

[15] R. E. Collin, *Antennas and Radiowave Propagation*. New York, NY, USA: McGraw-Hill, 1985.

[16] M. Burla, "Advanced integrated optical beamforming networks for broadband phased array antenna systems," Ph.D. dissertation, Univ. of Twente, Enschede, The Netherlands, 2013.

[17] T. H. Cormen, C. E. Leiserson, R. L. Rivest, and C. Stein, *Introduction to Algorithms*. Cambridge, MA, USA: MIT Press, 2001.

[18] L. Zhuang et al. *et al.*, "Low-loss, high-index-contrast Si_3N_4 SiO_2 optical waveguides for optical delay lines in microwave photonics signal processing," *Opt. Exp.*, vol. 19, no. 23, pp. 23162–23170, 2011.

[19] A. Meijerink, C. G. H. Roeloffzen, R. Meijerink, L. Zhuang, D. A. I. Marpaung, M. J. Bentum, M. Burla, J. Verpoorte, P. Jorna, A. Hulzinga, and W. van Etten, "Novel ring resonator-based integrated photonic beamformer for broadband phased array receive antennas—Part I: Design and performance analysis," *IEEE J. Lightw. Technol.*, vol. 28, no. 1, pp. 3–18, Jan. 2010.

[20] C. G. H. Roeloffzen, "Passband flattened binary-tree structured add-drop multiplexers using SiON waveguide technology," Ph.D. dissertation, Univ. of Twente, Enschede, The Netherlands, 2002.

[21] B. Verbeek C. H. Henry, N. A. Olsson, K. J. Orlowsky, R. F. Kazarinov, and B. H. Johnson, "Integrated four-channel Mach–Zehnder multi/demultiplexer fabricated with phosphorous doped SiO2 waveguides on Si," *IEEE J. Lightw. Technol.*, vol. 6, no. 6, pp. 1011–1015, Jun. 1988.

[22] M. Burla et al. *et al.*, "On-chip CMOS compatible reconfigurable optical delay line with separate carrier tuning for microwave photonic signal processing," *Opt. Exp.*, vol. 19, no. 22, pp. 21475–21484, 2011.

Maurizio Burla (S'08–M'12) was born in Orvieto, Italy, in 1982. He received the B.Sc. and M.Sc. degrees (*cum laude*) from the University of Perugia, Perugia, Italy, in 2005 and 2007, respectively. His M.Sc. thesis was developed at the University of Bristol, U.K., under the joint supervision of Prof. R. Sorrentino (University of Perugia, Italy) and Prof. M. Cryan (University of Bristol, U.K.), and dealt with the design and realization of planar multiband antennas based on fractal architecture for Wireless-over-Fiber transceiver applications.

From December 2006 to April 2007, he was intern at Delta-Utec Space Research and Consultancy, Leiden, The Netherlands, among the YES2 (Young Engineers Satellite 2) project, in the RF subsystem integration and testing. In December 2007, he joined the System Engineering group at AleniaSIA S.p.A., Torino, Italy, working on the avionic system of Alenia C-27J Spartan aircraft. From 2008 to 2012, he has worked at the Telecommunication Engineering Group, the University of Twente, Enschede, the Netherlands, as a Ph.D. student. His research focused on broadband optical beamformers based on integrated optical ring resonators, as part of the MEMPHIS project. Since October 2012, he has been a Postdoctoral Research fellow at INRS-EMT, Montréal, Canada, in the group of Prof. J. Azaña, working on integrated-waveguide technologies for ultrafast all-optical signal processing and microwave photonics.

Dr. Burla received the Best Paper Award at the 2013 IEEE International Topical Meeting on Microwave Photonics (MWP2013), October 28–31, 2013, Alexandria, Virginia, USA, and the Runner-up Student Award at the 2011 IEEE International Topical Meeting on Microwave Photonics (MWP2011), October 18–21, 2011, Singapore. His work has been selected to appear in the Research Highlights of the December 2011 Technology Focus of Nature Photonics. He was also a co-recipient of the second Best Student Team Award at the International Astronautical Congress 2008, Glasgow, Scotland, for his work in the YES2 project, and of the Best Poster Award at the MEMPHIS General Assembly 2008, Amersfoort, The Netherlands.

David A. I. Marpaung (S'05–M'xx) was born in Balikpapan, Indonesia, in 1979. He received the B.Sc. degree in physics (Hons.) from Institut Teknologi Bandung, Indonesia, in 2002, and the M.Sc. degree in applied physics and the Ph.D. degree in electrical engineering, both from the University of Twente, Enschede, The Netherlands, in 2003 and 2009, respectively. The topic of the Ph.D. thesis was the performance enhancement of analog photonic links. From August 2009 until July 2012, he was a Postdoctoral Researcher in the University of Twente within the framework of the European Commission FP7 funded project SANDRA. He was leading the research activities on microwave photonic system integration for a large-scale photonic beamformer in a phased array antenna system for satellite communications. Since August 2012, he has been a Research Fellow in the Centre for Ultrahigh Bandwidth Devices for Optical Systems (CUDOS), School of Physics, University of Sydney, Australia, working on photonic chip-based nonlinear signal processing for high speed coherent optical communication systems. His main research interests include the use of integrated photonic circuits for microwave photonic signal processing and high capacity optical communications.

Leimeng Zhuang (S'05) was born in Beijing, China, in 1980. He received the B.Sc. degree in telecommunication engineering from the University of Electronic Science and Technology of China, Chengdu, China, in June 2003, and the M.Sc. degree in electrical engineering (Hons.) and the Ph.D. degree in electrical engineering, both from the University of Twente, Enschede, The Netherlands, in June 2005 and November 2010, respectively. His Ph.D. thesis was about the true time delay-based broadband phased array antenna system comprising a photonic integrated beamformer using tunable ring resonator delay lines. From October 2009 until September 2010, he was working as a Product Specialist at XiO Photonics B.V., mainly involved in photonics integration and packaging. In the period from October 2010 until December 2013, he worked as a Research Fellow at the University of Twente, SATRAX B.V., and Dutch National Aerospace Laboratory, responsible for the development of a satellite tracking phased array antenna system. In March 2014, he joined the Electro-Photonics Interchange Laboratory, Electrical and Computer Systems Engineering, Monash University in Melbourne, Australia. He is currently a research fellow, working on the topic of a hybrid platform combining electronics and photonics for high-speed, energy-efficient optical communication systems and microwave photonics.

Muhammad Rezaul Khan (S'08) received the B.Sc. degree in engineering from the Islamic University of Technology, Gazipur, Bangladesh, in October 2002 (with distinction) and the M.Sc. degree in engineering from the Bangladesh University of Engineering and Technology, Dhaka, Bangladesh, in August 2006, both in electrical and electronics engineering.

He had served as a Lecturer in the Electrical and Electronics Engineering Department, Chittagong University of Engineering and Technology from June 2003 to July 2006. He also worked in ARSLOGICA s.r.l. Research Lab, and in the Embedded Electronics and Computing Systems Laboratory, University of Trento, Italy, from November 2006 to June 2008, as Research programs member.

Since July 2008, he is working toward the Ph.D. degree in the Telecommunication Engineering Group, the University of Twente, on Optical (de)multiplexing of radio signals, within the framework of the Smart Mix MEMPHIS (Merging Electronics and Micro and nano-PHotonics in Integrated Systems) project. His research is focused on the realization of components for antenna element steering at GHz frequencies, based on heterogeneous integration in Si-compatible technology, within the framework of the MEMPHIS project.

Arne Leinse was born in Enschede, The Netherlands, in 1977. He received the M.Sc. degree from the University of Twente, Integrated Optical Microsystems Group in 2001. In the same group, he started the Ph.D. work on the topic of active microring resonators for various optical applications. His Ph.D. work was carried out in the framework of a European project (IST 2000-28018 "Next generation Active Integrated optic Subsystems"') and his thesis was titled: "Polymeric microring resonator based electro-optic modulator." In 2005, he joined LioniX BV where he is now as a Project-/Account Manager involved in several integrated optical projects (e.g., the Senter Novem Smartmix Memphis project (Merging Electronics and Micro&nano-PHotonics in Integrated Systems) in which more than 20 partners participate.

Willem Beeker was born in Zwolle, The Netherlands, in 1980. He received the M.Sc. degree from the University of Twente in the laser physics and nonlinear optics group in 2004. In the same group, he started the Ph.D. work which resulted in the thesis: "*Nonlinear Scattering and Propagation of Ultrashort Pulses – Examples of Modeling and Applications*." In 2009, he joined Lionix BV where he worked as a Design Engineer on various projects and tasks included lithographic mask designs and optics modelling of waveguide structures. Since 2013, he joined Cambridge Design Partnership where he is employed as a Physicist and a Project Leader for product development in a variety fields including industrial, consumer, and medical devices.

Marcel Hoekman was born in Zutphen, The Netherlands, in 1974. He received the M.Sc. degree in applied physics and the MTD degree in integrated optics from the University of Twente, Enschede, The Netherlands, in 1998 and 2001, respectively. From 2004 to 2009, he has been a part time Ph.D. student at the Integrated Optical MicroSystems Group of the University of Twente, in the framework of the STW project "*Multi-Sensing Arrays of Separately Accessible Optics Sensors*."

From 1998 to 2001, he worked on his Postgraduate design program in the Integrated Optical MicroSystems Group, the University of Twente. He worked on the design of an integrated optical/electrooptical modulator based on PZT containing multilayer stacks. In this project, he worked together with the group Experimental Solid State Physics III, Radboud University Nijmegen. In 2001, he joined Lion Photonix Technologies BV, Enschede, The Netherlands—which has continued as LioniX B.V. since 2002—as a Design Engineer. Besides simulation and mask design, he has experience in several cleanroom manufacturing processes and characterization methods, and he has worked as Project Leader on several projects.

René G. Heideman was born in Goor, The Netherlands, in 1965. He received the M.Sc. and Ph.D. degrees in applied physics from the University of Twente, Enschede, The Netherlands, in August 1988 and January 1993, respectively. He is an expert in the field of MST, based on more than 20 years of experience. He specializes in integrated optics (IO), covering both (bio-) chemical sensing and telecom applications. He is (co)author of more than 150 papers and holds more than 20 patents in the IO-field, on 10 different subjects. Since 2001, he is the co-founder and CTO of LioniX BV. Since 2008, he is CTO of Panthera, a group a high-tech innovative companies focusing on creating new business based on micro/nanotechnology. He is Member of several Dutch steering committees and, among others, of IEEE BioPhotonics. He is also Board Member of MinacNed (association for microsystems and nanotechnology). Since June 2012, he is (visiting) Professor Nanotechnology of Saxion University of Applied Sciences.

Chris G. H. Roeloffzen (S'98–M'03) was born in Almelo, The Netherlands, in 1973. He received the M.Sc. degree in applied physics and Ph.D. degree in electrical engineering from the University of Twente, Enschede, The Netherlands, in 1998 and 2002, respectively.

From 1998 to 2002, he was engaged with research on integrated optical add-drop demultiplexers in Silicon Oxinitride waveguide technology, in the Integrated Optical Microsystems Group, the University of Twente. In 2002, he became an Assistant Professor in the Telecommunication Engineering Group, the University of Twente. He is now involved with research and education on microwave photonic systems. He is the Founder of the company SATRAX BV, a spin off of the University of Twente.